ELECTRONIC SUPPLEMENTARY INFORMATION

for the paper entitled

Complexation of some lanthanides(III), actinides and transition metal ions with a 6-(1,2,4-triazin-3-yl)-2,2':6',2''-terpyridine ligand: implications for actinide(III)/lanthanide(III) partitioning

Frank W. Lewis,*[a] Laurence M. Harwood,*[a] Michael J. Hudson,[a] Michael G. B. Drew,[a] Michal Sypula,[b] Giuseppe Modolo,[b] Daniel Whittaker,[c] Clint A. Sharrad,[c] Vladimira Videva,[d] Véronique Hubscher-Bruder[d] and Françoise Arnaud-Neu[d]

[a] *Department of Chemistry, The University of Reading, Whiteknights, Reading RG6 6AD, UK. E-mail: f.lewis@reading.ac.uk, l.m.harwood@reading.ac.uk*

[b] *Forschungszentrum Jülich GmbH, Sicherheitsforschung und Reaktortechnik, D-52425 Jülich, Germany. E-mail: g.modolo@fz-juelich.de*

[c] *The Mill-C40, School of Chemical Engineering and Analytical Science, The University of Manchester, Manchester M13 9PL, UK. E-mail: clint.a.sharrad@manchester.ac.uk*

[d] *Université de Strasbourg, IPHC, 25 Rue Becquerel, 67087 Strasbourg, France – CNRS, UMR 7178, 67037 Strasbourg, France. E-mail: veronique.hubscher@unistra.fr*

CONTENTS **PAGE**

1: Experimental Procedures

General procedures

Melting points were obtained on a Stuart SMP10 instrument. IR spectra were recorded as Nujol® mulls (N) on a Perkin Elmer RX1 FT-IR instrument. ^{1}H, ^{13}C−{^{1}H} and ^{13}C NMR spectra were recorded using either a Bruker AMX400 or an Avance DFX400 instrument. Chemical shifts are reported in parts per million downfield from tetramethylsilane. Assignments were verified with ^{1}H-^{1}H and ^{1}H-^{13}C COSY experiments as appropriate. Mass spectra were obtained under electrospray conditions on a Thermo Scientific LTQ Orbitrap XL instrument. Elemental microanalyses were carried out by Medac Ltd., Brunel Science Centre, Surrey (UK). All organic reagents were obtained from either Acros or Aldrich, while inorganic reagents were obtained from either BDH or Aldrich and used as received.

2,2':6',2''-Terpyridine-1-oxide 4[1–5]

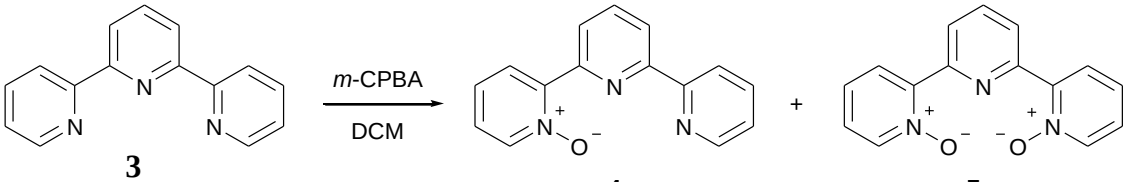

3 **4** **5**

2,2':6',2''-Terpyridine **3** (5.02 g, 21.52 mmol) was dissolved in DCM (150 mL) and a solution of *m*-CPBA (4.82 g, 77 %, 21.52 mmol, 1 eq) in DCM (200 mL) was added. The solution was stirred at room temperature for 24 hours. The solution was diluted with DCM (50 mL) and then washed with 10 % sodium carbonate solution (2 × 100 mL), dried over magnesium sulfate and evaporated to afford a yellow solid (5.61 g). The crude product was purified by column chromatography on silica gel, eluting first with 5 % MeOH in DCM, then with 25 % MeOH in DCM to afford three products. The first product to elute was unchanged **3** as a yellow solid (1.32 g, 26 %). The second product to elute was **4** as a yellow solid (2.81 g, 52 %). ^{1}H NMR (249.8 MHz; $CDCl_3$, Me_4Si): δ 7.24–7.35 (2H, m, 5-H and 5''-H), 7.39 (1H, td, *J* = 7.6 and 1.2, 4-H), 7.82 (1H, td, *J* = 7.8 and 1.7, 4''-H), 7.96 (1H, t, *J* = 7.9, 4'-H), 8.32–8.38 (2H, m, 3-H and 6-H), 8.47 (2H, d, *J* = 7.9, 5'-H and 3''-H), 8.69 (1H, d, *J* = 4.7, 6''-H), 8.98 (1H, d, *J* = 7.9, 3'-H) ppm. The third product to elute was the corresponding bis-*N*-oxide **5**[1,6–10] as a white solid (0.78 g, 13 %). ^{1}H NMR (249.8 MHz; $CDCl_3$, Me_4Si): δ 7.27–7.34 (2H m, 5-H and 5''-H), 7.39 (2H, td, *J* = 7.7 and 1.3, 4-H and 4''-H), 7.98 (1H, t, *J* =

7.9, 4’-H), 8.19 (2H, dd, *J* = 7.8 and 2.2, 3-H and 3’’-H), 8.35 (2H, dd, *J* = 6.3 and 1.2, 6-H and 6’’-H), 8.93 (2H, d, *J* = 8.0, 3’-H and 5’-H) ppm.

2,2':6',2''-Terpyridine-6-carbonitrile 6[3,11–13]

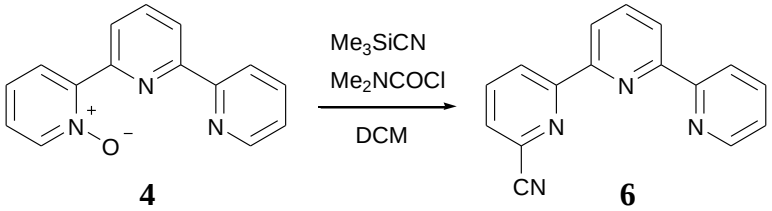

4 **6**

The starting material **4** (2.81 g, 11.28 mmol) was dissolved in DCM (150 mL) and trimethylsilyl cyanide (2.11 mL, 16.92 mmol, 1.5 eq) was added. *N*,*N*-Dimethylcarbamyl chloride (1.56 mL, 16.92 mmol, 1.5 eq) was added and the solution was stirred at room temperature for 3 days. The solution was diluted with DCM (50 mL) and then 10 % potassium carbonate solution (100 mL) was added. The solution was vigorously stirred for 15 minutes during which time effervesence occurred. The phases were separated and the aqueous layer was extracted with DCM (2 × 50 mL). The combined organic layers were dried over magnesium sulfate and evaporated to afford a brown semi-solid (5.03 g) which was purified by column chromatography on silica gel, eluting with 5 % MeOH in DCM to afford **6** as a white solid (2.71 g, 93 %). ^{1}H NMR (249.8 MHz; $CDCl_3$, Me_4Si): δ 7.36 (1H, ddd, *J* = 7.5, 4.8 and 1.1, 4’’-H), 7.73 (1H, dd, *J* = 7.6 and 1.0, 5’-H), 7.87 (1H, td, *J* = 7.7 and 1.7, 5’’-H), 8.00 (2H, td, *J* = 7.8 and 1.4, 4-H and 4’-H), 8.51 (2H, dd, *J* = 7.7 and 1.0, 3-H and 5-H), 8.57 (1H, d, *J* = 7.9, 6’’-H), 8.70–8.73 (1H, m, 3’’-H), 8.87 (1H, dd, *J* = 8.1 and 1.0, 3’-H) ppm. ^{13}C NMR (62.8 MHz; $CDCl_3$; Me_4Si): δ 117.4 (*C*N), 121.1 (C-6’’), 121.5 (C-5’), 122.0 (C-3’), 122.1 (C-5), 124.0 (C-3), 124.3 (C-4’’), 128.1 (C-5’’), 128.2 (C-3’’), 136.9 (C-4’), 137.8 (C-4), 138.2 (quat), 149.2 (quat), 153.2 (quat), 155.6 (quat), 155.8 (quat) ppm.

2,2':6',2''-Terpyridine-6-carbohydrazonamide 7[11,14–15]

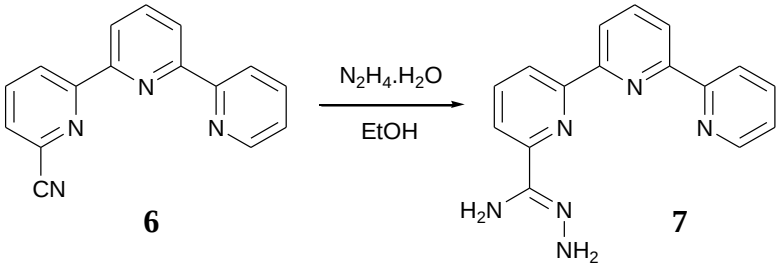

6 **7**

To a suspension of **6** (2.71 g, 10.50 mmol) in EtOH (50 mL) was added hydrazine hydrate (25 mL, 64 %). The suspension was stirred at room temperature for 12 days. Water (500 mL) was added and the precipitated solid was filtered and washed with water (200 mL) and allowed to dry in the air to afford **7** as a white solid (1.50 g, 49 %). ^{1}H NMR (249.8 MHz; $CDCl_3$, Me_4Si): δ 4.65 (2H, br s, N*H*$_2$), 5.44 (2H, br s, N*H*$_2$), 7.35 (1H, ddd, *J* = 7.5, 4.7 and 1.2, 4’’-H), 7.84–7.92 (2H, m, 4’-H and 5’’-H), 7.98 (1H, t, *J* = 7.8, 4-H), 8.08 (1H, dd, *J* = 7.8 and 1.0, 6’’-H), 8.47 (2H, d, *J* = 7.8, 3’-H and 5’-H), 8.63 (2H, d, *J* = 7.8, 3-H and 5-H), 8.70–8.73 (1H, m, 3’’-H) ppm.

2: X-ray Crystallography

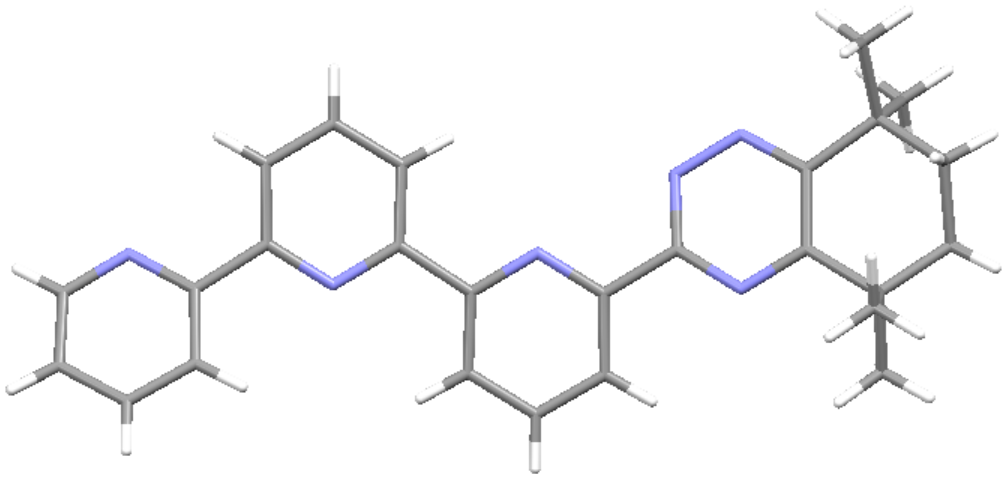

Figure 13. Mercury plot of $CyMe_4$-hemi-BTBP **2**. CCDC 869235 contains the crystallographic data for this structure. These data can be obtained free of charge via www.ccdc.cam.ac.uk/conts/retrieving.html, or from the Cambridge Crystallographic Data Centre, 12 Union Road, Cambridge CB2 1EZ, UK (fax: (+44)1223-336-033; or deposit@ccdc.cam.ac.uk).

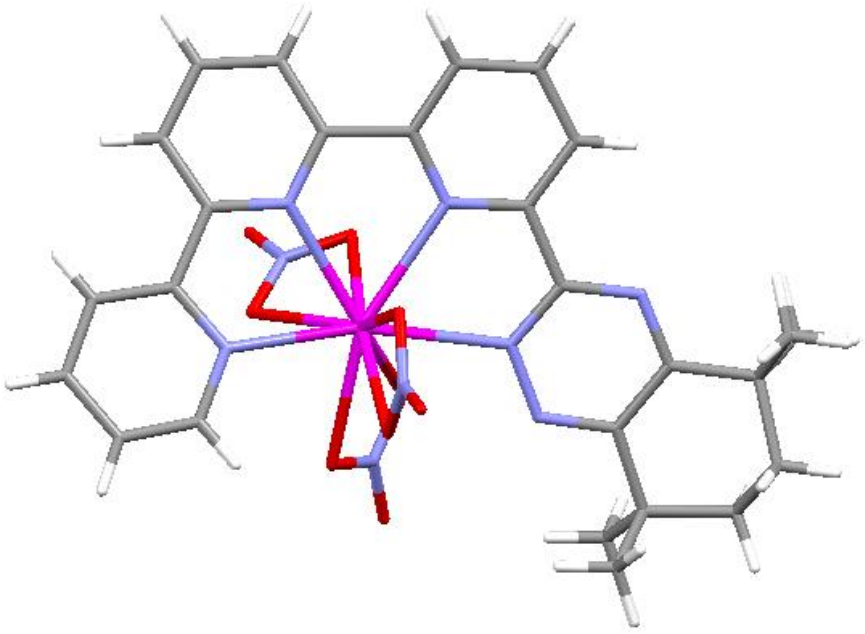

Figure 14. Mercury plot of [Eu(**2**)$(NO_3)_3$].2MeCN. Solvent molecules omitted for clarity. CCDC 869234 contains the crystallographic data for this structure. These data can be obtained free of charge via www.ccdc.cam.ac.uk/conts/retrieving.html, or from the Cambridge Crystallographic Data Centre, 12 Union Road, Cambridge CB2 1EZ, UK (fax: (+44)1223-336-033; or deposit@ccdc.cam.ac.uk).

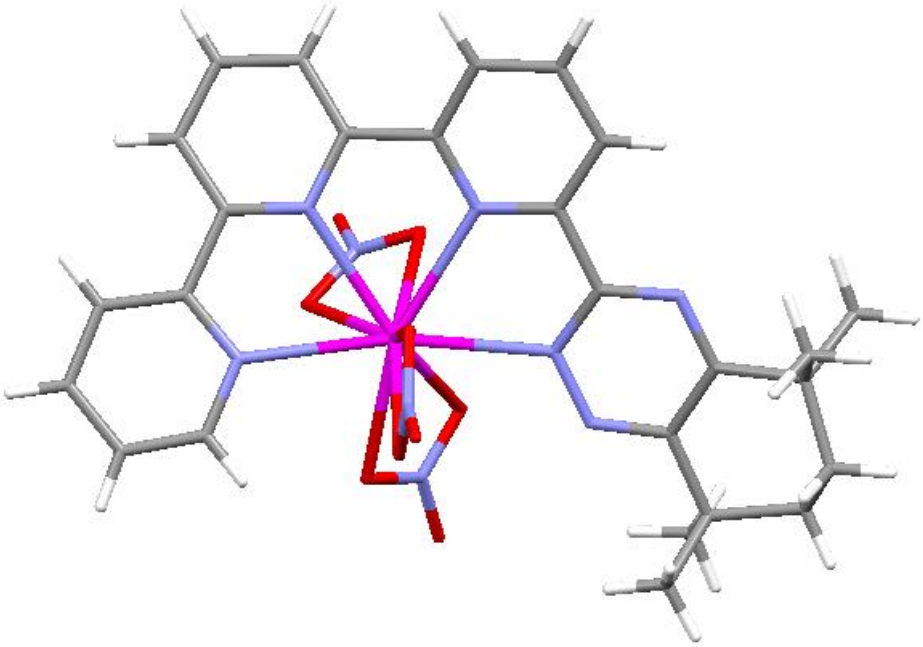

Figure 15. Mercury plot of [Ce(**2**)$(NO_3)_3$].C_7H_8. Solvent molecules omitted for clarity. CCDC 869233 contains the crystallographic data for this structure. These data can be obtained free of charge via www.ccdc.cam.ac.uk/conts/retrieving.html, or from the Cambridge Crystallographic Data Centre, 12 Union Road, Cambridge CB2 1EZ, UK (fax: (+44)1223-336-033; or deposit@ccdc.cam.ac.uk).

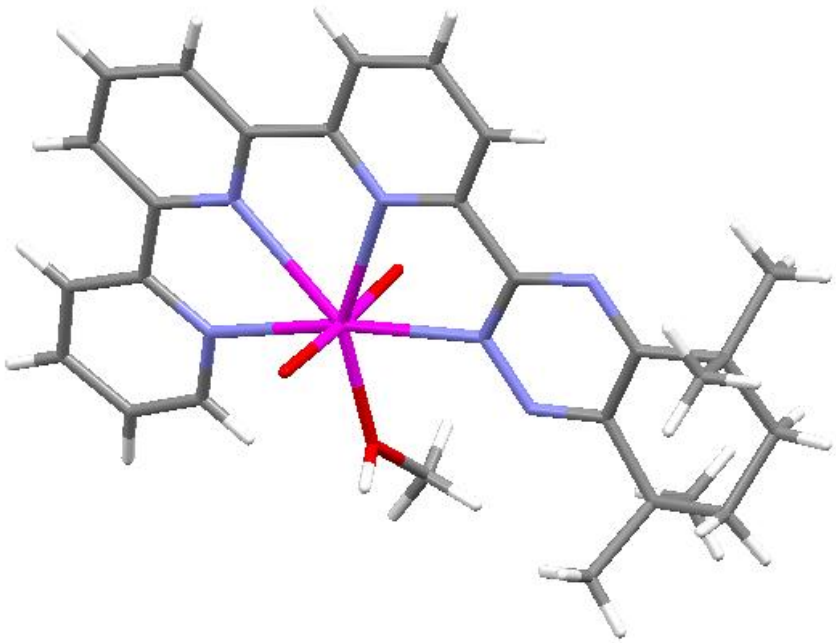

Figure 16. Mercury plot of $[UO_2(\mathbf{2})MeOH][UO_2(NO_3)_4]$. Counterion omitted for clarity. CCDC 869236 contains the crystallographic data for this structure. These data can be obtained free of charge via www.ccdc.cam.ac.uk/conts/retrieving.html, or from the Cambridge Crystallographic Data Centre, 12 Union Road, Cambridge CB2 1EZ, UK (fax: (+44)1223-336-033; or deposit@ccdc.cam.ac.uk).

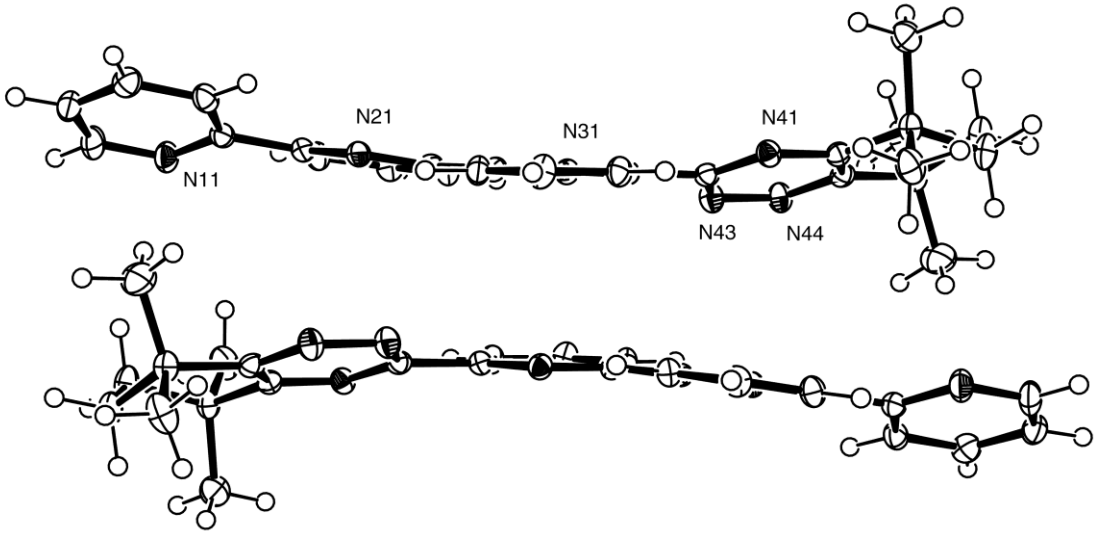

Figure 17. The packing of two molecules of $CyMe_4$-hemi-BTBP **2** across a centre of symmetry showing the π-π stacking, particularly between the central pyridine rings.

3: Solvent Extraction Studies

Table 1. Extraction of Am(III) and Eu(III) by $CyMe_4$-hemi-BTBP **2** (0.01 M) + 2-bromohexanoic acid (1 M) into 1-octanol as a function of initial nitric acid concentration (*D* = distribution ratio, SF = separation factor, contact time: 60 min, temperature: 22 °C ± 1 °C).

[HNO_3]	D_{Am}	D_{Eu}	$SF_{Am/Eu}$
0.001	1.343 ± 0.067	0.089 ± 0.018	15.0 ± 0.8
0.005	0.497 ± 0.025	0.032 ± 0.006	15.0 ± 0.8
0.01	0.145 ± 0.007	0.010 ± 0.002	15.0 ± 0.8
0.05	0.0109 ± 0.0022	0.0016 ± 0.0003	7.0 ± 0.4
0.1	0.0054 ± 0.0011	0.00020 ± 0.00004	27.0 ± 1.4
0.2	0.0021 ± 0.0004	0.0010 ± 0.0002	2.0 ± 0.1

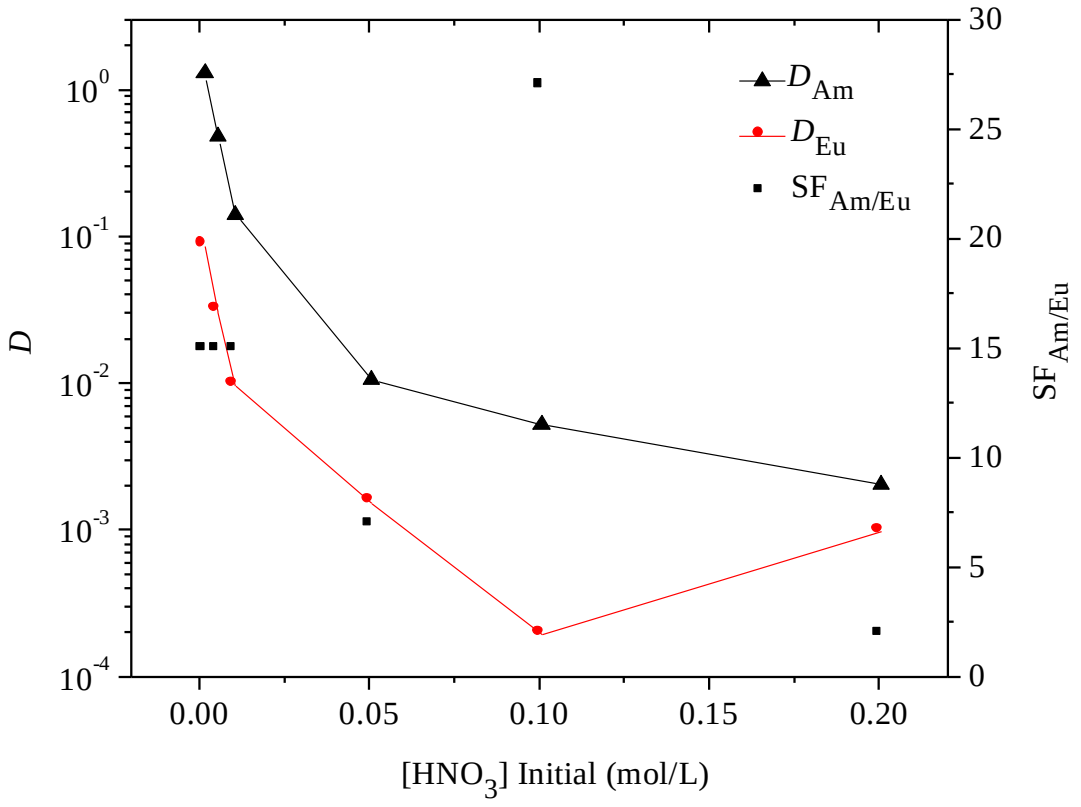

Figure 18. Extraction of Am(III) and Eu(III) by $CyMe_4$-hemi-BTBP **2** (0.01 M) + 2-bromohexanoic acid (1 M) into 1-octanol as a function of initial nitric acid concentration (*D* = distribution ratio, SF = separation factor, ▲ = D_{Am}, ● = D_{Eu}, ■ = $SF_{Am/Eu}$, contact time: 60 min, temperature: 22 °C ± 1 °C).

4: NMR Titrations with Metal Salts

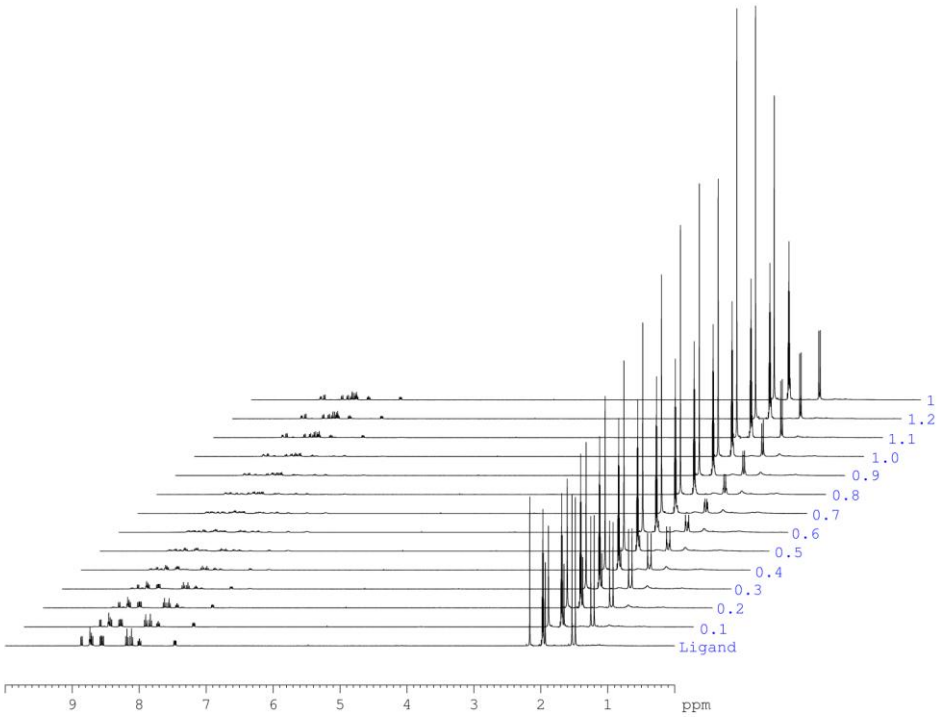

Figure 19. Stack plot for the ^{1}H NMR titration of CyMe$_4$-hemi-BTBP **2** with La(NO$_3$)$_3$ in CD$_3$CN. Bottom spectrum = free ligand. Each preceeding spectrum corresponds to the addition of 0.1 equivalents of metal salt solution. Peaks at 1.97 ppm and 2.15 ppm due to solvent.

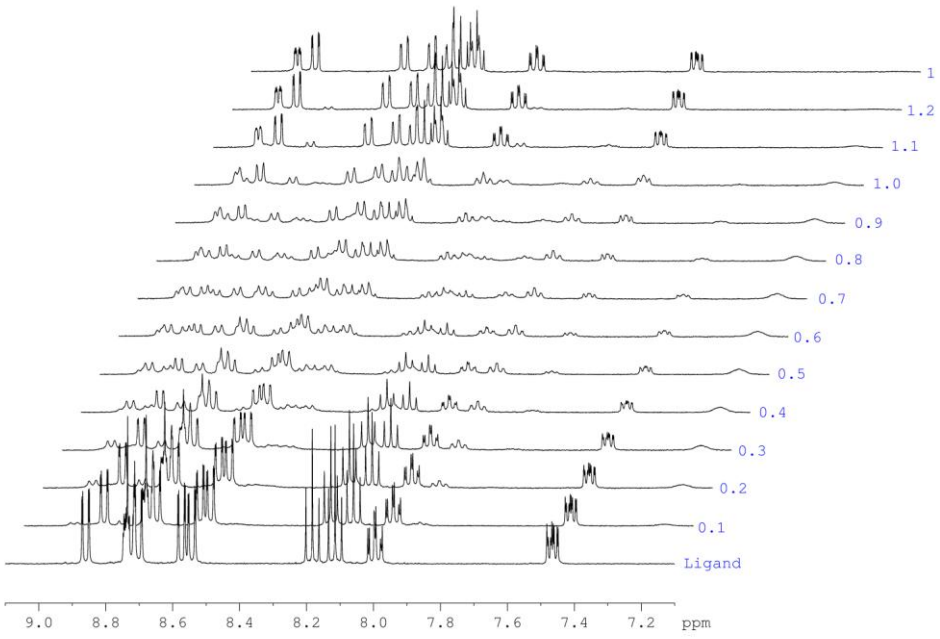

Figure 20. Aromatic region of the stack plot for the ^{1}H NMR titration of $CyMe_4$-hemi-BTBP **2** with $La(NO_3)_3$ in CD_3CN. Bottom spectrum = free ligand. Each preceeding spectrum corresponds to the addition of 0.1 equivalents of metal salt solution.

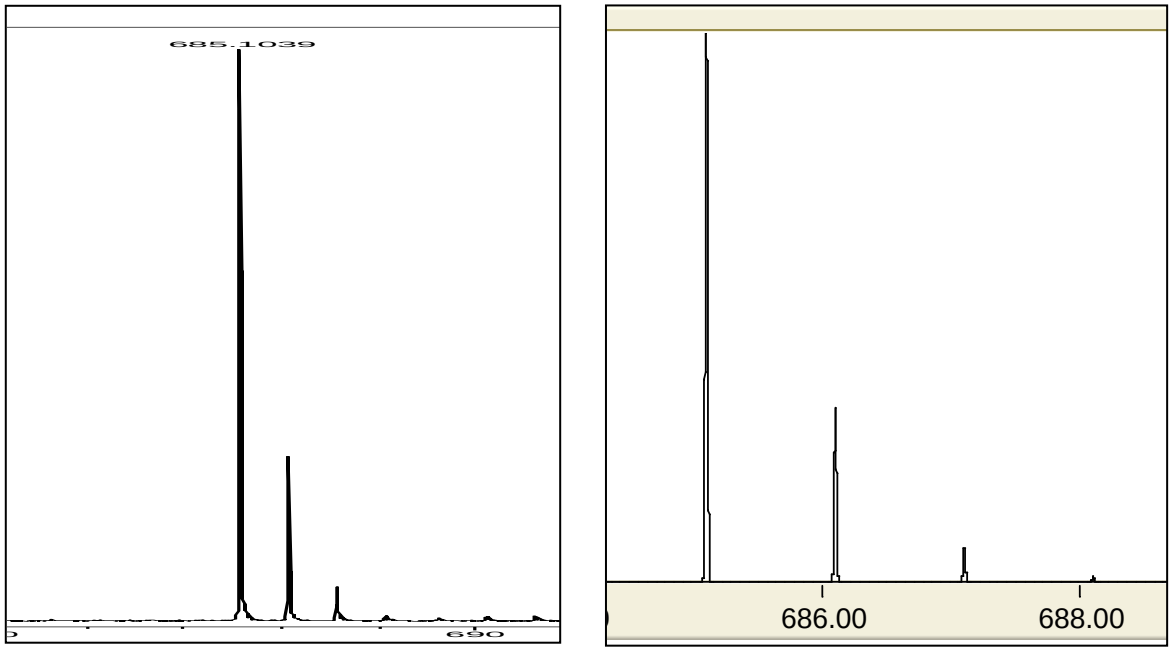

Figure 21. Left: Enlargement of the electrospray-ionization mass spectrum of the final solution species formed during the titration of $CyMe_4$-hemi-BTBP **2** with $La(NO_3)_3$. The mass peak at m/z = 685.1039 corresponds to $[La(\mathbf{2})(NO_3)_2]^+$. Right: Computer simulation of the isotope distribution pattern of $[La(\mathbf{2})(NO_3)_2]^+$.

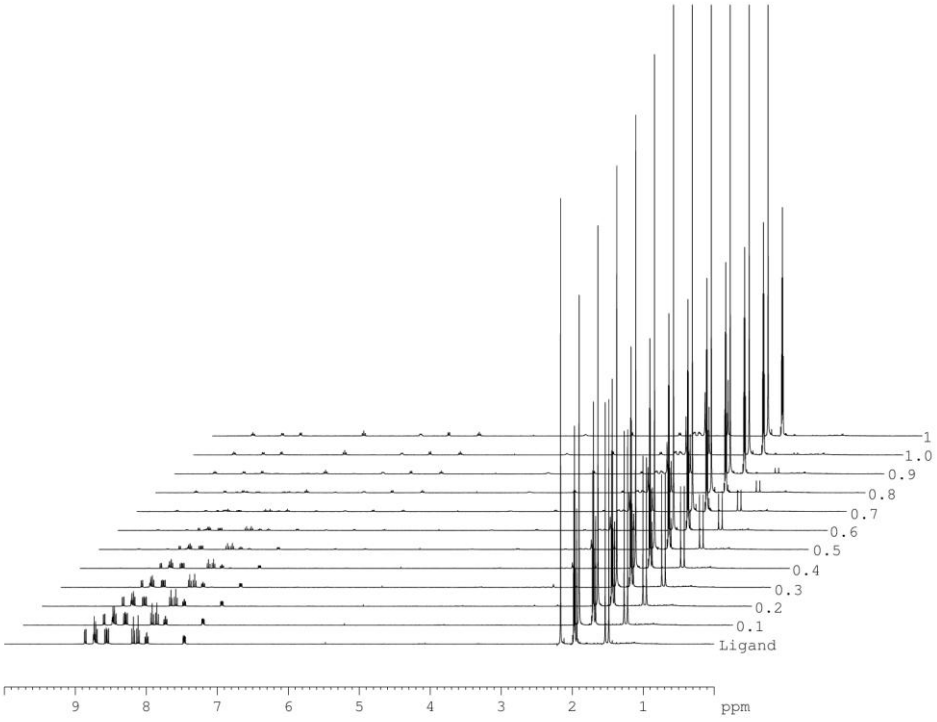

Figure 22. Stack plot for the ^{1}H NMR titration of $CyMe_4$-hemi-BTBP **2** with $Eu(NO_3)_3$ in CD_3CN. Bottom spectrum = free ligand. Each preceeding spectrum corresponds to the addition of 0.1 equivalents of metal salt solution. Peaks at 1.97 ppm and 2.15 ppm due to solvent.

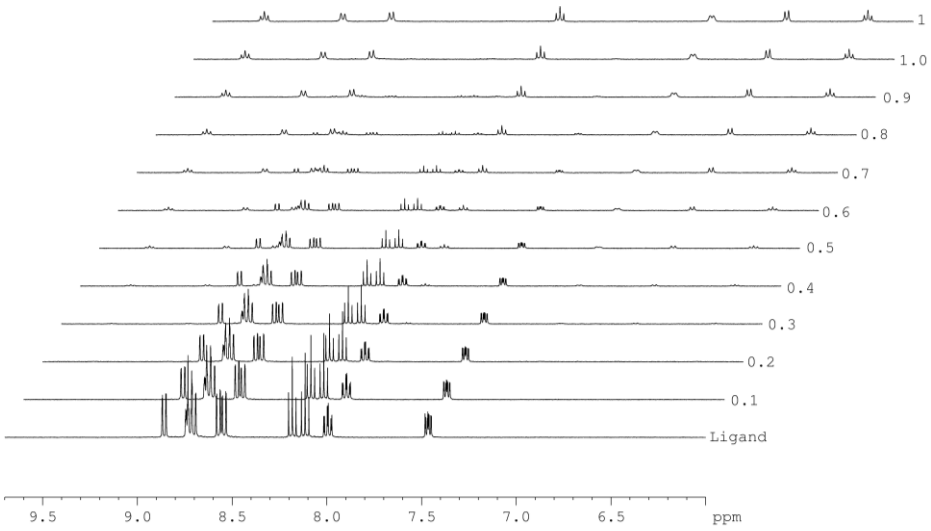

Figure 23. Aromatic region of the stack plot for the ^{1}H NMR titration of CyMe$_4$-hemi-BTBP **2** with Eu(NO$_3$)$_3$ in CD$_3$CN. Bottom spectrum = free ligand. Each preceeding spectrum corresponds to the addition of 0.1 equivalents of metal salt solution.

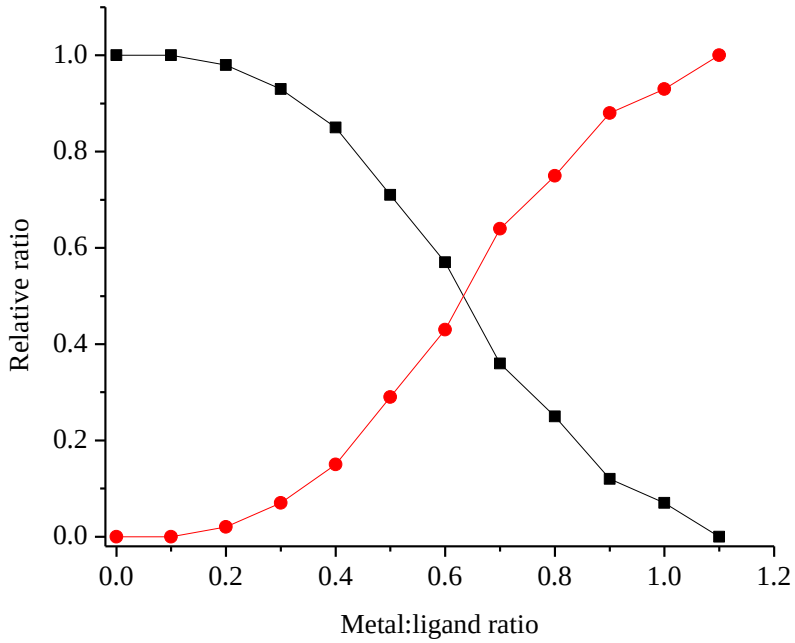

Figure 24. ^{1}H NMR titration of CyMe$_4$-hemi-BTBP **2** with Eu(NO$_3$)$_3$ in CD$_3$CN (■ = free ligand, ● = 1:1 complex).

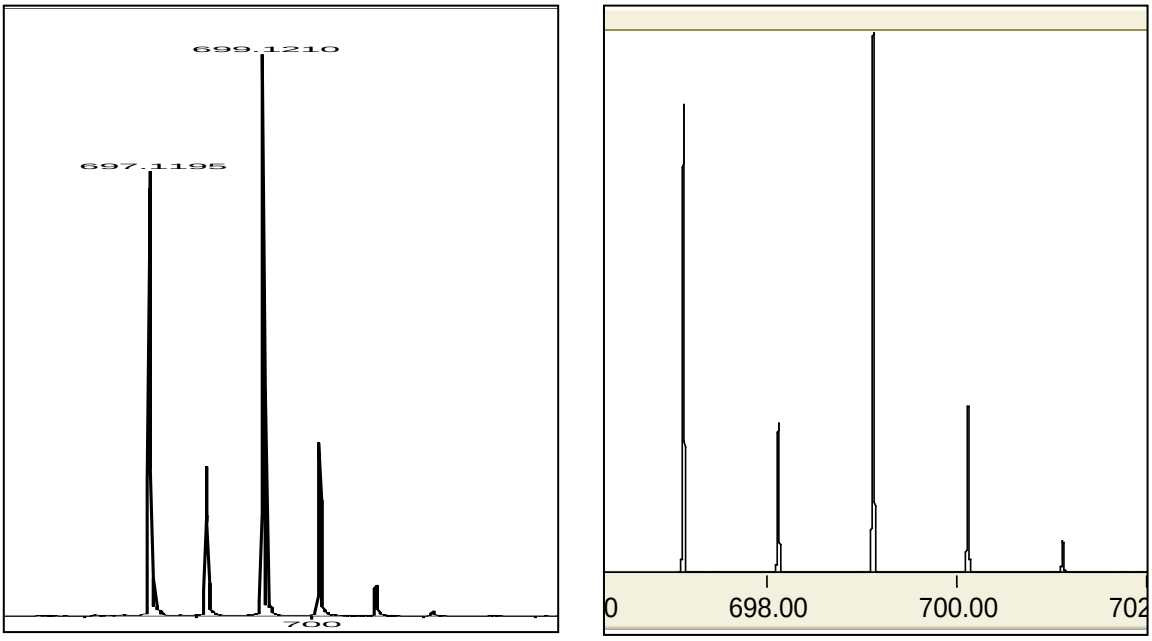

Figure 25. Left: Enlargement of the electrospray-ionization mass spectrum of the final solution species formed during the titration of $CyMe_4$-hemi-BTBP **2** with $Eu(NO_3)_3$. The mass peak at m/z = 699.1210 corresponds to $[Eu(\mathbf{2})(NO_3)_2]^+$. Right: Computer simulation of the isotope distribution pattern of $[Eu(\mathbf{2})(NO_3)_2]^+$.

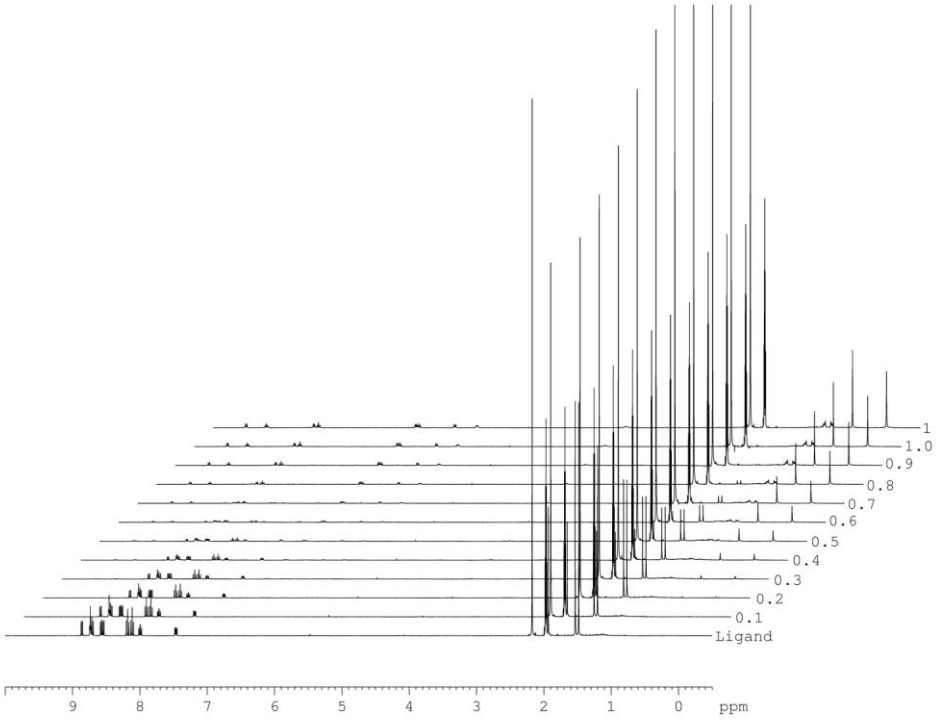

Figure 26. Stack plot for the ^{1}H NMR titration of $CyMe_4$-hemi-BTBP **2** with $Ce(NO_3)_3$ in CD_3CN. Bottom spectrum = free ligand. Each preceeding spectrum corresponds to the addition of 0.1 equivalents of metal salt solution. Peaks at 1.97 ppm and 2.15 ppm due to solvent.

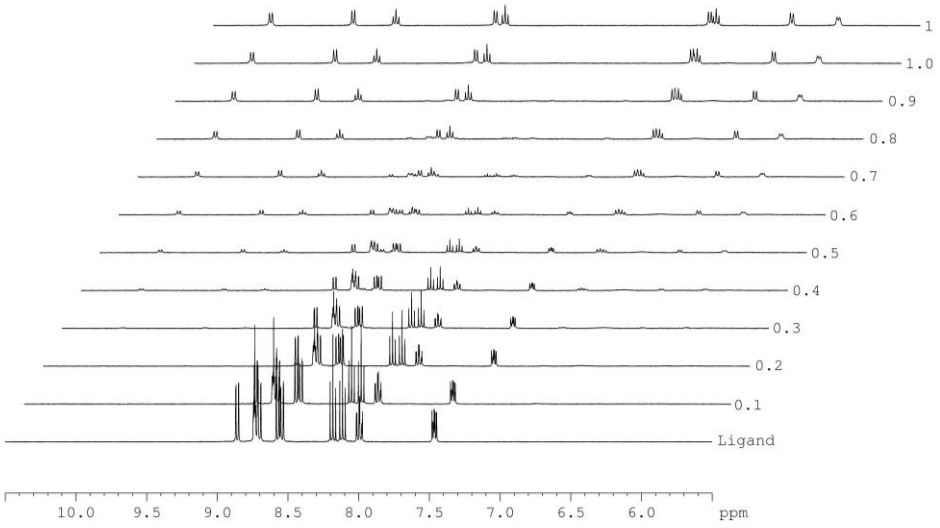

Figure 27. Aromatic region of the stack plot for the ^{1}H NMR titration of CyMe$_4$-hemi-BTBP **2** with $Ce(NO_3)_3$ in CD_3CN. Bottom spectrum = free ligand. Each preceeding spectrum corresponds to the addition of 0.1 equivalents of metal salt solution.

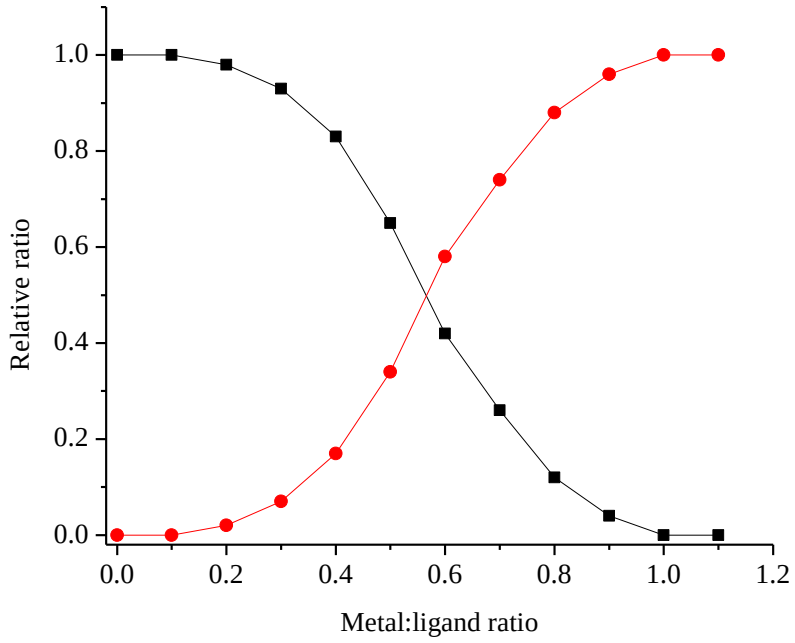

Figure 28. ^{1}H NMR titration of CyMe$_4$-hemi-BTBP **2** with $Ce(NO_3)_3$ in CD_3CN (■ = free ligand, ● = 1:1 complex).

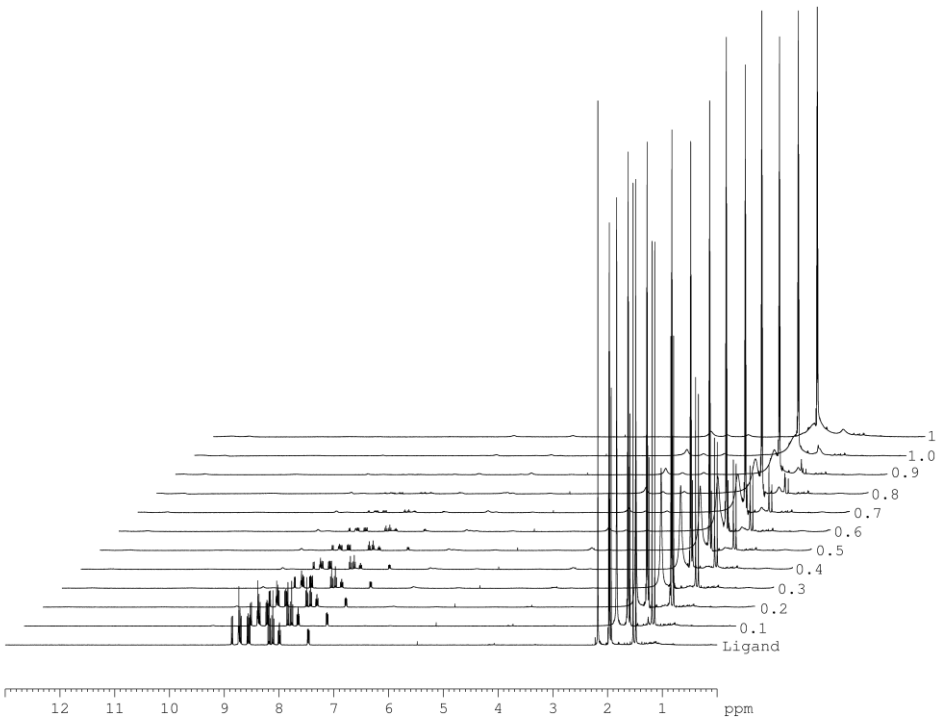

Figure 29. Stack plot for the ^{1}H NMR titration of $CyMe_4$-hemi-BTBP **2** with $Yb(NO_3)_3$ in CD_3CN. Bottom spectrum = free ligand. Each preceeding spectrum corresponds to the addition of 0.1 equivalents of metal salt solution. Peaks at 1.97 ppm and 2.15 ppm due to solvent.

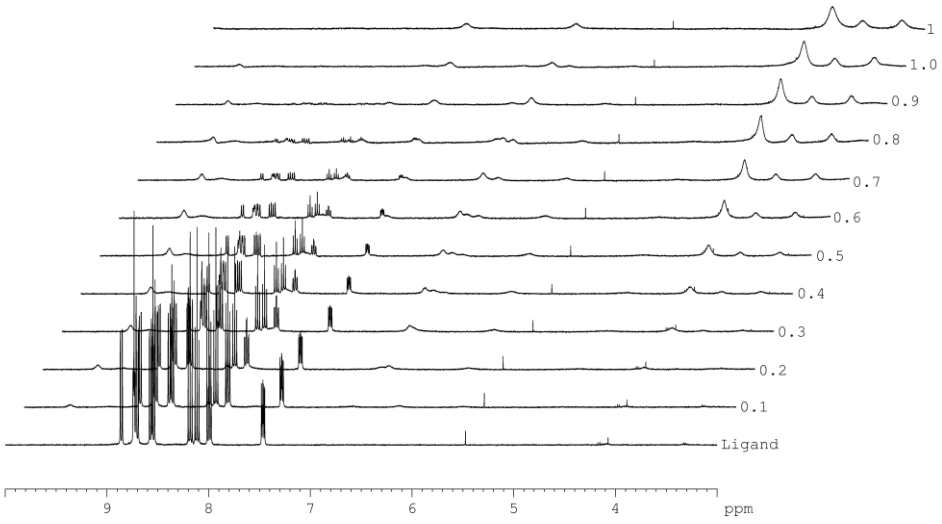

Figure 30. Enlargement of the region from 3 ppm to 10 ppm of the Stack plot for the ^{1}H NMR titration of $CyMe_4$-hemi-BTBP **2** with $Yb(NO_3)_3$ in CD_3CN. Bottom spectrum = free ligand. Each preceeding spectrum corresponds to the addition of 0.1 equivalents of metal salt solution.

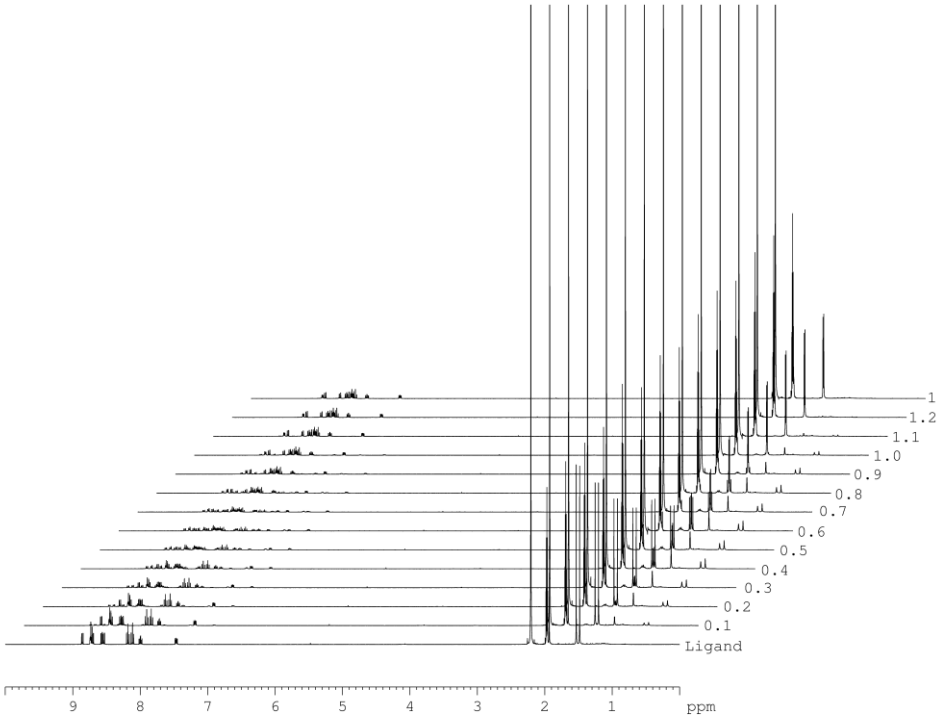

Figure 31. Stack plot for the ^{1}H NMR titration of $CyMe_4$-hemi-BTBP **2** with $Y(NO_3)_3$ in CD_3CN. Bottom spectrum = free ligand. Each preceeding spectrum corresponds to the addition of 0.1 equivalents of metal salt solution. Peaks at 1.97 ppm and 2.15 ppm due to solvent.

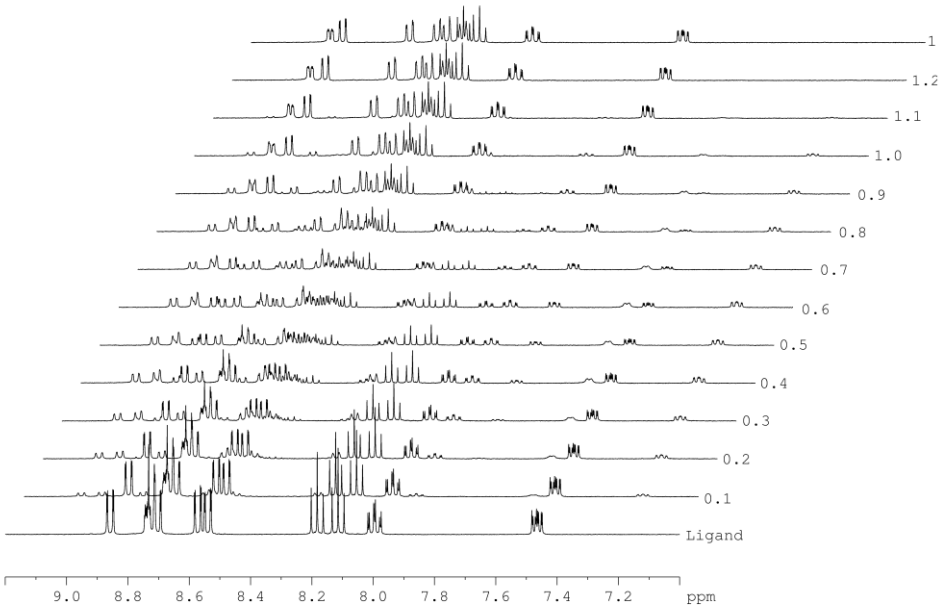

Figure 32. Aromatic region of the stack plot for the ^{1}H NMR titration of $CyMe_4$-hemi-BTBP **2** with $Y(NO_3)_3$ in CD_3CN. Bottom spectrum = free ligand. Each preceeding spectrum corresponds to the addition of 0.1 equivalents of metal salt solution.

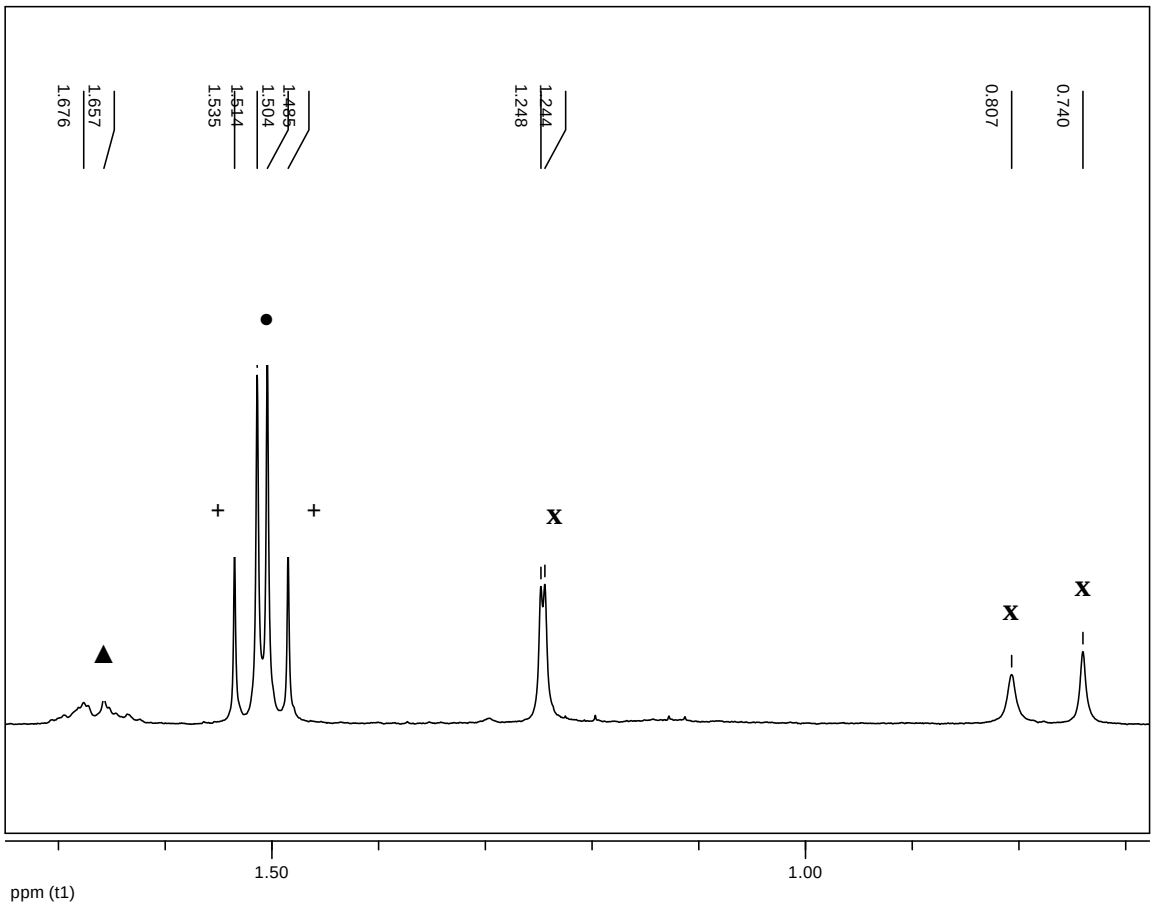

Figure 33. Aliphatic region of ^{1}H NMR spectrum of CyMe$_4$-hemi-BTBP **2** in CD_3CN after 0.7 equivalents of $Y(NO_3)_3$ have been added (Assignments: + = methyl groups of the free ligand, ● = methyl groups of the 1:1 complex, x = methyl groups of the chiral 1:2 complex, ▲ = methylene protons of the chiral 1:2 complex).

Explanation of the chirality of 1:2 bis-complexes of $CyMe_4$-hemi-BTBP 2 with $Y(NO_3)_3$

In the free ligand **2**, two methyl peaks are observed in the ^{1}H NMR spectrum because the two sets of gem-dimethyl groups are not symmetrically equivalent due to the non-symmetry of the 1,2,4-triazine ring in **2**. When a bis-complex of **2** is formed with a lanthanide (not cosidering an additional nitrate ion in the inner coordination sphere at this point), this leads to two possible C2-symmetric complexes which are enantiomeric and therefore chiral. This chirality effectively desymmetrises each gem-dimethyl group in the ligand **2**, therefore each methyl group in each ligand **2** in the bis-complex will give a 3-proton singlet in the NMR spectrum, hence 4 methyl peaks overall (due to the C2-symmetry, each ligand can be interchanged with the other ligand in the bis-complex, hence the two ligands are equivalent). The situation becomes more complicated when an additional nitrate ion is included in the inner sphere of the bis-complex (see Figure 34 below). Addition of a nitrate ion to each enantiomer of the bis-complex can take place from 4 possible directions as shown (north east, north west, south west and south east) giving structures 1–8 (Figure 34).

The nitrate ion can attack with 3 possible orientations; along the C2 axis *anti* to the bulky aliphatic $CyMe_4$-part of each ligand (north west), along the C2 axis *syn* to the aliphatic $CyMe_4$-part of each ligand (south east) or at a 90 degree angle to the C2 axis of the bis-complex (north east and south west). Inspection of structures 1–8 shows that 1 is enantiomeric with 6, 2 is enantiomeric with 5, 3 is enantiomeric with 8 and 4 is enantiomeric with 7. Further inspection shows that 1 is the same as 3 and 6 is the same as 8. In other words, 3 diastereomers of the bis-complex with an inner sphere nitrate ion are possible, each one is a racemic mixture of enantiomers. The three diastereomers are 2/5, 4/7 and 1/6.

Structures 2 and 5 (resulting from attack *anti* to the $CyMe_4$-parts) are C2 symmetric as they have an axis of symmetry bisecting the two $CyMe_4$-parts and going through the nitrate ligand. Each ligand in 2 and 5 can thus be interchanged with the other, hence the methyl groups are equivalent. Thus 4 methyl peaks would be expected in the ^{1}H NMR spectrum for this diastereomer.

Similarly, structures 4 and 7 (resulting from attack *syn* to the $CyMe_4$-parts) are C2 symmetric with an axis of symmetry bisecting the two $CyMe_4$-parts and going through the nitrate ligand. Thus 4 methyl peaks would also be expected in the ^{1}H NMR spectrum for this diastereomer.

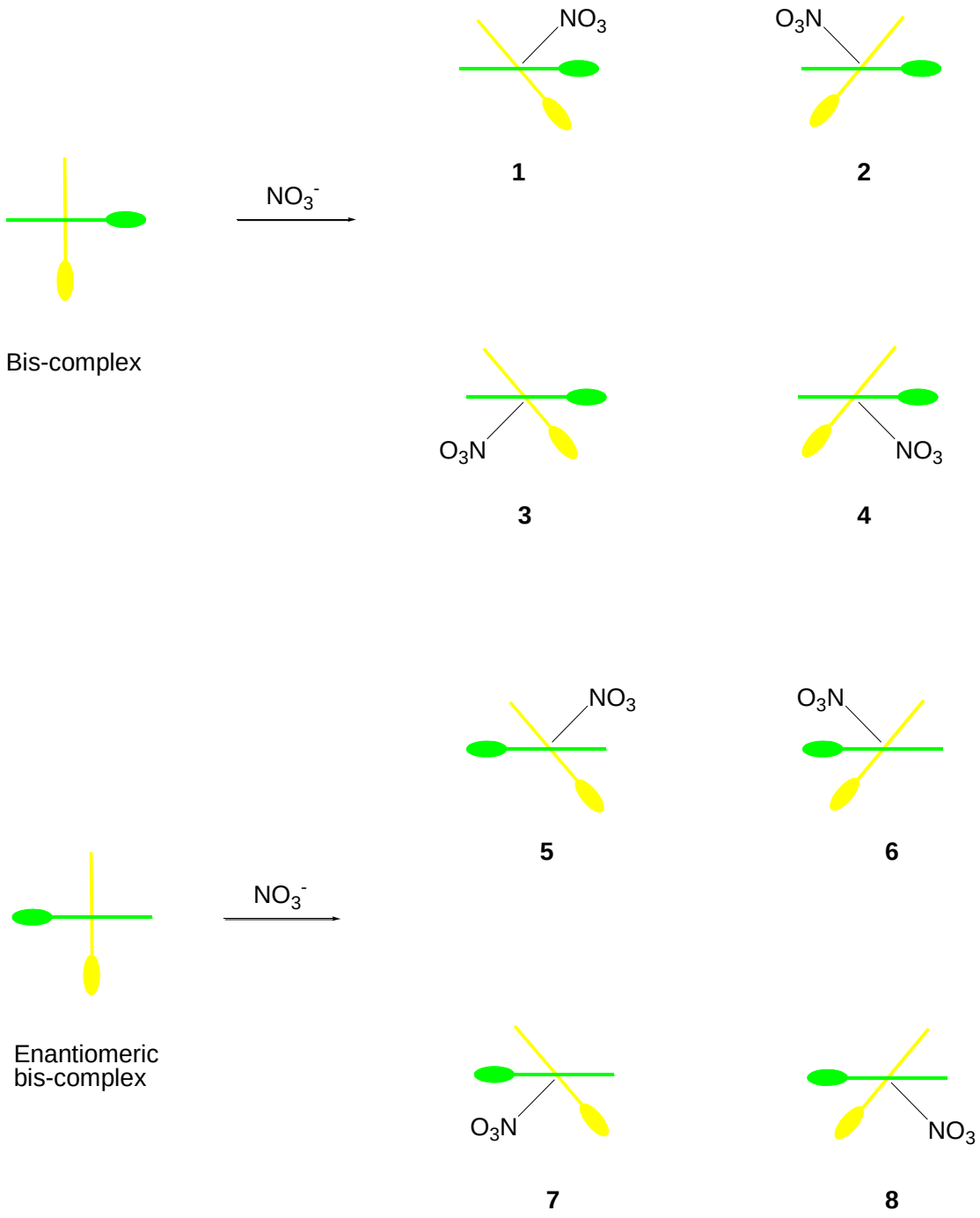

Figure 34. Possible diastereomeric bis-complexes formed by $CyMe_4$-hemi-BTBP **2** with trivalent lanthanide nitrates.

Structures 1/3 and 6/8 (resulting from attack at a 90 degree angle to the C2 axis of the bis-complex) do not have an axis of symmetry, therefore each ligand in these structures cannot be interchanged with the other. It is further obvious that the $CyMe_4$-parts of each ligand are not the same; one is close to the nitrate ligand while the other is farther away. Therefore 4 methyl peaks would be expected for each ligand in the bis-complex (ie: 8 overall).

In summary, two of the 3 possible diastereomers of the bis-complex containing a nitrate ligand in the inner coordination sphere will give 4 methyl peaks in the NMR spectrum while the third should give 8 methyl peaks. It appears that only a single diastereomer of the bis-complex is being formed in the present case as we observe only 4 methyl peaks in our NMR experiments with Y. We propose that it is probably structures 2/5 on steric grounds (the nitrate ligand is farthest away from the bulky $CyMe_4$-parts and the two $CyMe_4$-parts are farther away from each other). Structures 4/7 are probably least likely on steric grounds, since the nitrate ion is closest to the $CyMe_4$-parts. Of course the bis-complexes of the ligand with an additional nitrate ion could also be fluxional so that all ligands arrange around the metal so as to form the sterically most stable bis-complex (probably structures 2/5).

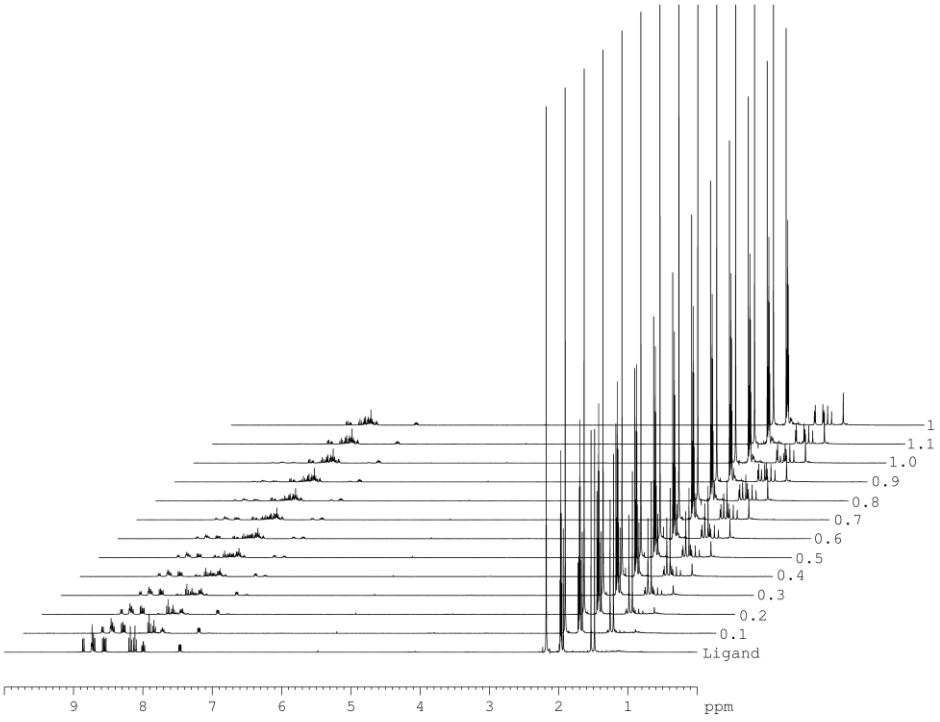

Figure 35. Stack plot for the ^{1}H NMR titration of $CyMe_4$-hemi-BTBP **2** with $CuBF_4$ in CD_3CN. Bottom spectrum = free ligand. Each preceeding spectrum corresponds to the addition of 0.1 equivalents of metal salt solution. Peaks at 1.97 ppm and 2.15 ppm due to solvent.

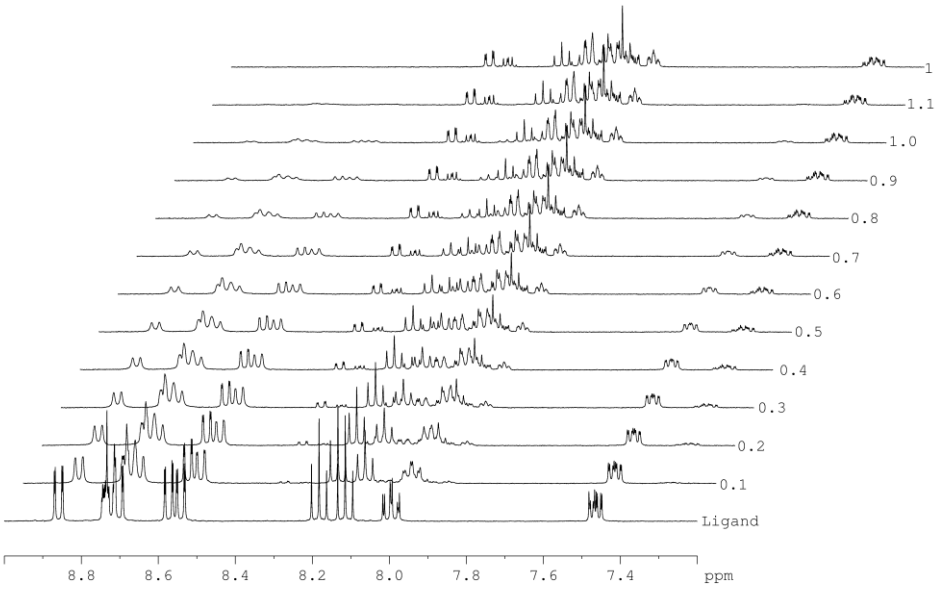

Figure 36. Aromatic region of the stack plot for the ^{1}H NMR titration of $CyMe_4$-hemi-BTBP **2** with $CuBF_4$ in CD_3CN. Bottom spectrum = free ligand. Each preceeding spectrum corresponds to the addition of 0.1 equivalents of metal salt solution.

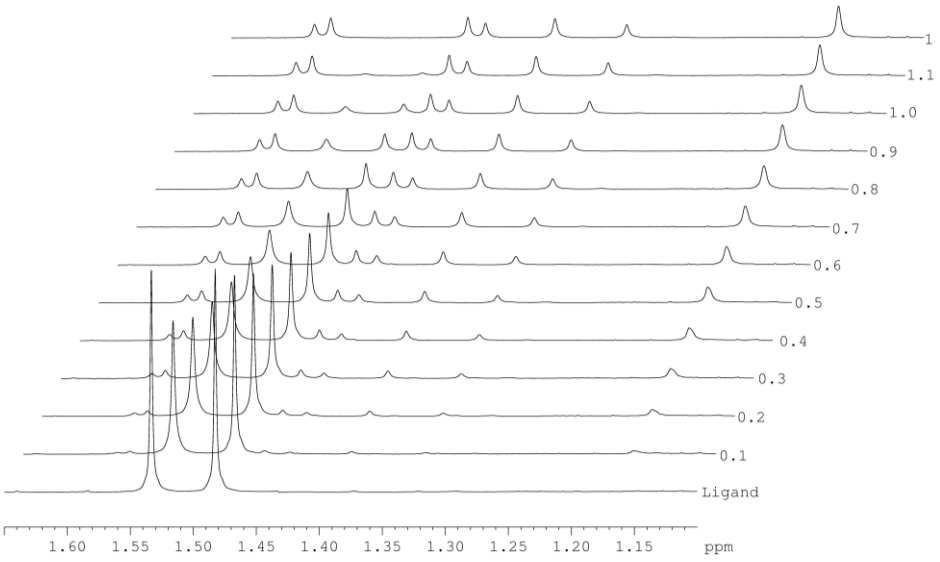

Figure 37. Aliphatic region of the stack plot for the ^{1}H NMR titration of CyMe$_4$-hemi-BTBP **2** with $CuBF_4$ in CD_3CN. Bottom spectrum = free ligand. Each preceeding spectrum corresponds to the addition of 0.1 equivalents of metal salt solution.

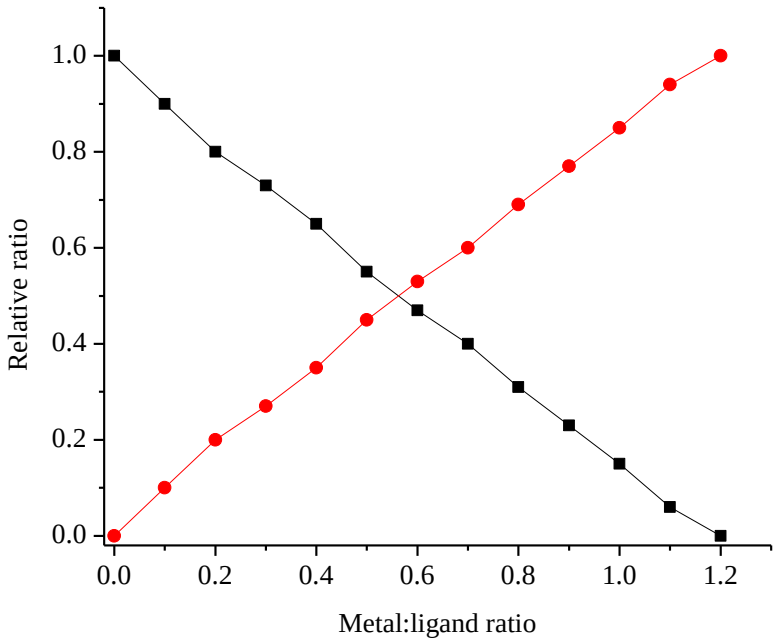

Figure 38. ^{1}H NMR titration of CyMe$_4$-hemi-BTBP **2** with $CuBF_4$ in CD_3CN (■ = free ligand, ● = 2:2 complex).

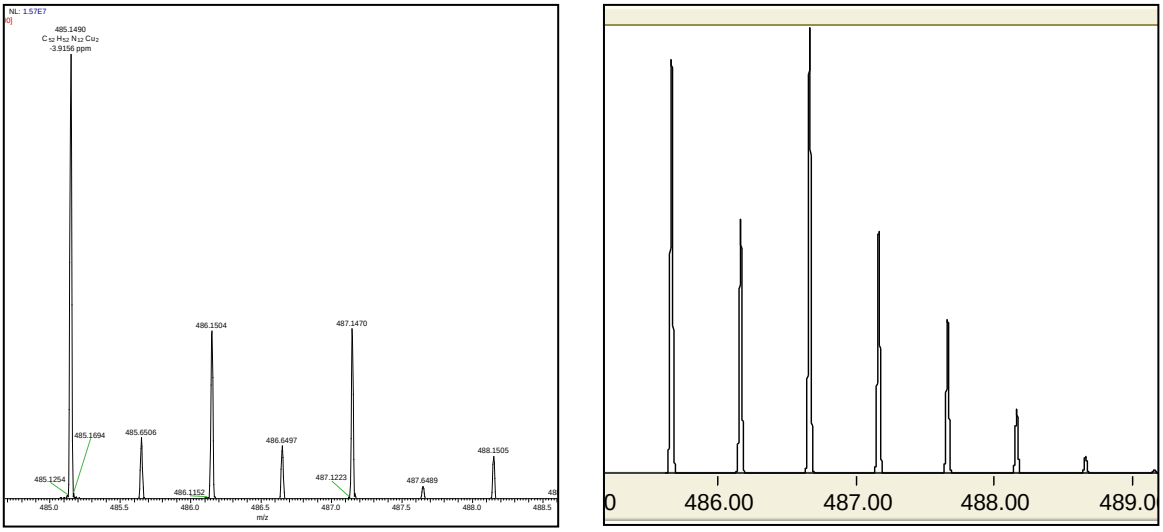

Figure 39. Left: Enlargement of the electrospray-ionization mass spectrum of the final solution species formed during the titration of $CyMe_4$-hemi-BTBP **2** with $[Cu(MeCN)_4BF_4]$. The mass peak at m/z = 485.1490 corresponds to $[Cu_2(\mathbf{2})_2]^{2+}$. Right: Computer simulation of the isotope distribution pattern of $[Cu_2(\mathbf{2})_2]^{2+}$.

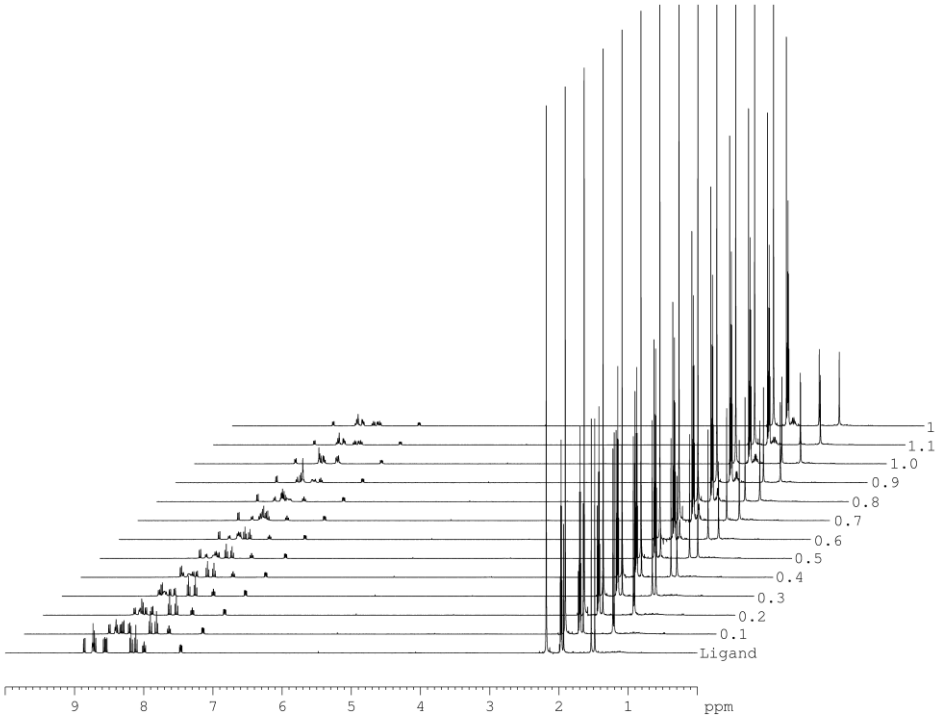

Figure 40. Stack plot for the ^{1}H NMR titration of $CyMe_4$-hemi-BTBP **2** with $AgBF_4$ in CD_3CN. Bottom spectrum = free ligand. Each preceeding spectrum corresponds to the addition of 0.1 equivalents of metal salt solution. Peaks at 1.97 ppm and 2.15 ppm due to solvent.

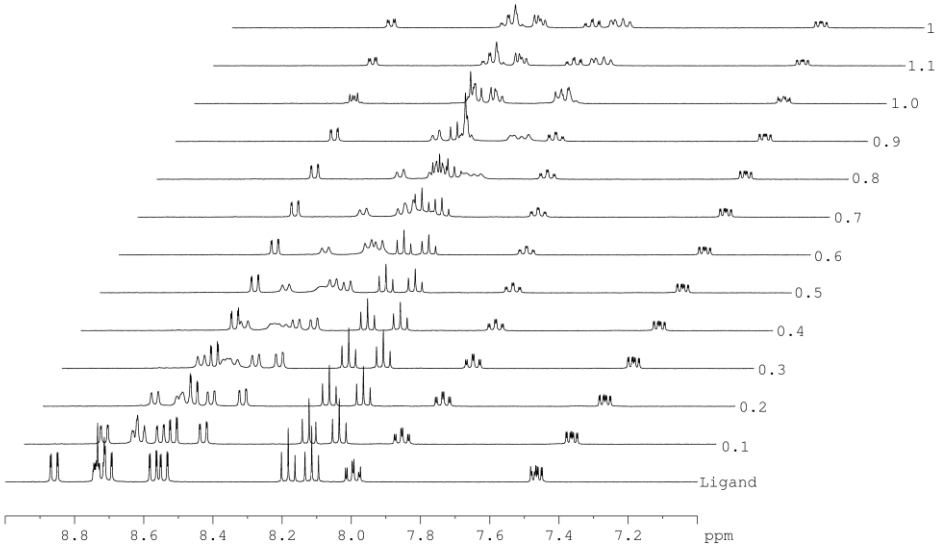

Figure 41. Aromatic region of the stack plot for the ^{1}H NMR titration of $CyMe_4$-hemi-BTBP **2** with $AgBF_4$ in CD_3CN. Bottom spectrum = free ligand. Each preceeding spectrum corresponds to the addition of 0.1 equivalents of metal salt solution.

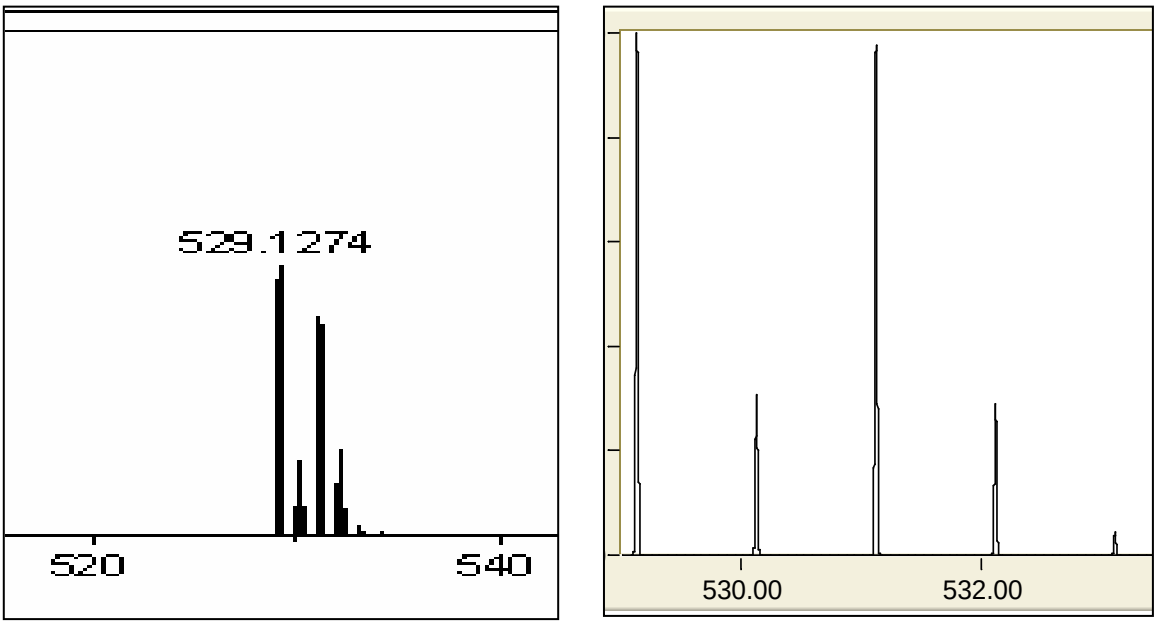

Figure 42. Left: Enlargement of the electrospray-ionization mass spectrum of the final solution species formed during the titration of $CyMe_4$-hemi-BTBP **2** with $[Ag(MeCN)_4BF_4]$. The mass peak at m/z = 529.1274 corresponds to $[Ag(\mathbf{2})]^+$. Right: Computer simulation of the isotope distribution pattern of $[Ag(\mathbf{2})]^+$.

5: References

1. R. P. Thummel, Y. Jahng, *J. Org. Chem.* **1985**, *50*, 3635.
2. A. J. Amoroso, M. W. Burrows, A. A. Dickinson, C. Jones, D. J. Willock, W.-T. Wong, *J. Chem. Soc. Dalton Trans.* **2001**, 225.
3. C. R. Rice, C. J. Baylies, H. J. Clayton, J. C. Jeffrey, R. L. Paul, M. D. Ward, *Inorg. Chim. Acta* **2003**, *351*, 207.
4. A. J. Amoroso, M. W. Burrows, R. Haigh, M. Hatcher, M. Jones, U. Kynast, K. M. A. Malik, D. Sendor, *Dalton Trans.* **2007**, 1630.
5. A. J. Amoroso, M. W. Burrows, S. J. Coles, R. Haigh, R. D. Farley, M. B. Hursthouse, M. Jones, K. M. A. Malik, D. M. Murphy, *Dalton Trans.* **2008**, 506.
6. C. Galaup, J.-M. Couchet, S. Bedel, P. Tisnès, C. Picard, *J. Org. Chem.* **2005**, *70*, 2274.
7. V. M. Mukkala, C. Sund, M. Kwiatkowski, P. Pasanen, M. Hogberg, J. Kankare, H. Takalo, *Helv. Chim. Acta* **1992**, *75*, 1621.
8. K. Ito, T. Nagata, K. Tanaka, *Inorg. Chem.* **2001**, *40*, 6331.
9. S. E. McKay, J. A. Sooter, S. G. Bodige, S. C. Blackstock, *Heterocyclic Commun.* **2001**, *7*, 307.
10. E. S. Andreiadis, R. Demadrille, D. Imbert, J. Pecaut, M. Mazzanti, *Chem.–Eur. J.* **2009**, *15*, 9458.
11. G. R. Pabst, J. Sauer, *Tetrahedron* **1999**, *55*, 5067.
12. F. R. Heirtzler, *Synlett* **1999**, 1203.
13. F. Heirtzler, M. Neuburger, K. Kulike, *J. Chem. Soc. Perkin Trans. 1.* **2002**, 809.
14. G. R. Pabst, J. Sauer, *Tetrahedron Lett.* **1998**, *39*, 6687.
15. G. R. Pabst, O. C. Pfüller, J. Sauer, *Tetrahedron Lett.* **1998**, *39*, 8825.